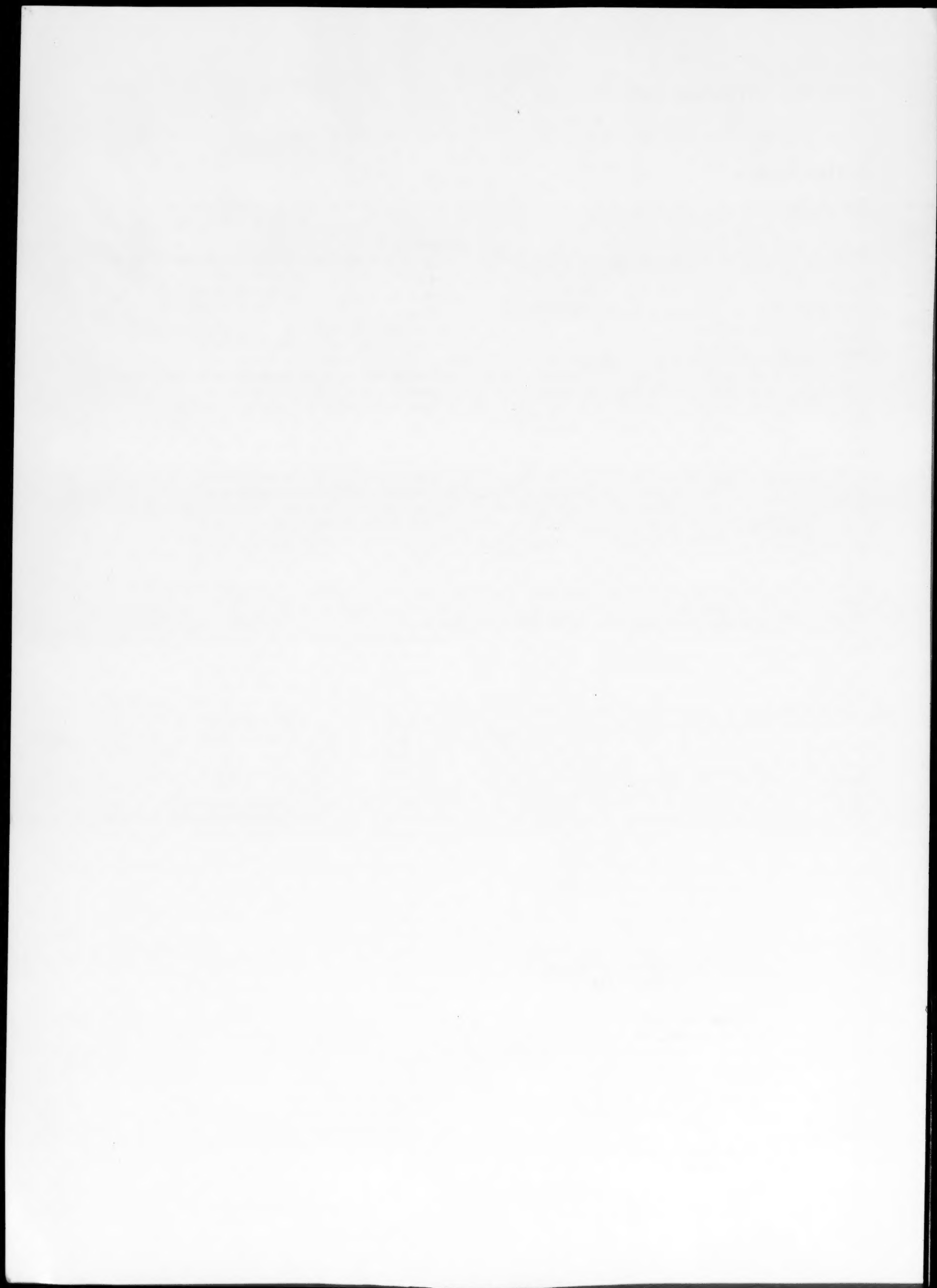


Author Index

- Arridge, R. G. C., 125
- Bang, K., L1
- Barrera, E. V., 45
- Benci, J. E., 51
- Birringer, R., 33
- Blucher, J., L1
- Cădek, J., L5
- Chao, P. T., 191
- Chen, N.-P., 157
- Christ, H.-J., L25
- Chumbley, L. S., 59
- Cizeron, G., 175
- Cornie, J. A., 199
- Cotterell, B., 149
- De Angelis, R. J., 75
- Delamore, G. W., 255
- Do'Hi, T., 227
- Downing, H. L., 59
- Duan, J. Z., 3
- Dybiec, H., L31
- Edmonds, D. V., 67
- Fisher, R. M., 3
- Fox, A. G., 3
- Froes, F. H., 19
- Gan, D., 141
- Gibson, M. A., 255
- Giessen, B. C., L1
- Greenwood, G. W., L21
- Gross, T. S., 75
- Grujicic, M., 215
- Heald, S. M., 45
- Hsueh, C.-H., 115
- Hu, C. T., 247
- Hu, Z. Q., 221
- Inal, O. T., 167
- Jackson, A. G., 11
- Jones, H., L21
- Kaesche, H., L1
- Kao, P.-W., 143
- Ke, Y.-B., 149
- Kim, Y.-W., 19
- Korbel, A., L31
- Kostorz, G., L17
- Kozubski, R., L17
- Krishnamurthy, S., 19
- Kwon, H., 133
- Laird, C., 83, 95, 103
- Leu, S. S., 247
- Li, Q., 199
- Li, Y. Y., 221
- Liang, F.-L., 83, 95, 103
- Liu, J., 221
- Lu, M.-C., 115
- Mai, Y.-W., 149
- Maier, H. J., L11
- Marcus, H. L., 45
- Masur, L. A., 199
- Mathews, V. K., 75
- Megusar, J., 199
- Michalek, A., L17
- Mishra, R. S., L21
- Miyamoto, Y., 207
- Mukherjee, K., 167
- Murakami, K., 207, 227
- Nakazono, S., 207
- Okamoto, T., 207, 227
- Okazaki, K., 75
- Omlor, R. E., 11
- Pak, H.-R., 167
- Pak, J. S. L., 167
- Paruz, H., 67
- Plumtree, A., 157
- Pope, D. P., 51
- Ren, J.-C., 235
- Robertson, E., 11
- Schwander, P., L17
- Servant, C., 175
- Shen, P., 191
- Soltys, J., L17
- Song, J. S., 133
- Spitzig, W. A., 59
- Tang, N.-Y., 157
- Todd, J. A., 235
- Verhoeven, J. D., 59
- Yao, K.-F., 157
- You, R. K., 141



Subject Index

Aging

- dynamic strain aging in Czochralski-grown silicon single crystals, 75

Alloys

- investigation into the structural evolutions of a low alloy steel during tempering, 175
- phase transformations in (Ni,Cu)₃Sn alloys, 167
- plastic deformation: a major factor in hydrogen embrittlement of low alloy steel, L11
- rapid solidification and self-annealing of Fe-C-Si alloys by low pressure plasma spraying, 207
- rapid solidification of lightweight metal alloys, 19
- rapidly solidified thick deposit layers of Fe-C-Mo alloys by flame spraying, 227
- the mechanism of superplastic flow in an Al-Mg alloy, L31

Aluminium

- a high resolution transmission electron microscopy study of SiC-coated graphite fiber-aluminum composite, 199
- mechanical properties of Fe-30Mn-10Al-1C-1Si alloy, 141
- morphology of zirconia in Y-PSZ sintered with Ni₂AlTi, 191
- the mechanism of superplastic flow in an Al-Mg alloy, L31
- up-quenching effect on the stabilization process of a Cu-Zn-Al martensite, 247

Annealing

- rapid solidification and self-annealing of Fe-C-Si alloys by low pressure plasma spraying, 207

Austenite

- the effect of cold work on the precipitation kinetics of an advanced austenitic steel, 235

Boron

- crystallization of low silicon content Fe-Si-B metallic glasses, 255

Carbon

- a high resolution transmission electron microscopy study of SiC-coated graphite fiber-aluminum composite, 199
- coherent precipitation of M₂C carbides in AF1410 steel, 215
- effects of nickel additions on the fracture behavior of tempered martensite in medium-carbon 6W steel, 133
- mechanical properties of Fe-30Mn-10Al-1C-1Si alloy, 141
- rapid solidification and self-annealing of Fe-C-Si alloys by low pressure plasma spraying, 207
- rapidly solidified thick deposit layers of Fe-C-Mo alloys by flame spraying, 227

Cavity growth

- on the cavity-growth-model-based prediction of the stress dependence of time to creep fracture, L5

Cold working

- the effect of cold work on the precipitation kinetics of an advanced austenitic steel, 235

Composites

- a high resolution transmission electron microscopy study of SiC-coated graphite fiber-aluminum composite, 199
- electron microscopy observation of an *in situ* Cu-Nb composite, 59
- the thermal expansion of a two-phase composite with body-centred cubic symmetry, 125

Copper

- control of intergranular fatigue cracking by slip homogeneity in copper
 - I: effect of grain size, 95
 - II: effect of loading mode, 103
- electron microscopy observation of an *in situ* Cu-Nb composite, 59
- microradiography of creep damage in copper, 51
- phase transformations in (Ni,Cu)₃Sn alloys, 167
- preparation of the metastable interstitial copper nitride, Cu₄N, by d.c. plasma ion nitriding, L1
- the effect of environment on the mechanism of fatigue crack initiation and propagation in polycrystalline copper, 83
- up-quenching effect on the stabilization process of a Cu-Zn-Al martensite, 247

Cracking

- control of intergranular fatigue cracking by slip homogeneity in copper
 - I: effect of grain size, 95
 - II: effect of loading mode, 103
- on the orientation of cyclic-slip-induced intergranular fatigue cracks in face-centred cubic metals, L21
- the effect of environment on the mechanism of fatigue crack initiation and propagation in polycrystalline copper, 83

Creep

- microradiography of creep damage in copper, 51
- on the cavity-growth-model-based prediction of the stress dependence of time to creep fracture, L5

Crystallization

- crystallization of low silicon content Fe-Si-B metallic glasses, 255

Czochralski growth

- dynamic strain aging in Czochralski-grown silicon single crystals, 75

Deformation

- plastic deformation: a major factor in hydrogen embrittlement of low alloy steel, L11

Diffusion

- some correlations between parameters relating to grain boundary self-diffusion in silver, L21

Embrittlement

- effect of directional solidification on resistance to hydrogen embrittlement of a stainless steel, 221
- plastic deformation: a major factor in hydrogen embrittlement of low alloy steel, L11

Fatigue

- control of intergranular fatigue cracking by slip homogeneity in copper
- I: effect of grain size, 95
- II: effect of loading mode, 103
- on the orientation of cyclic-slip-induced intergranular fatigue cracks in face-centred cubic metals, L25
- the effect of environment on the mechanism of fatigue crack initiation and propagation in polycrystalline copper, 83

Fracture

- effects of nickel additions on the fracture behavior of tempered martensite in medium-carbon 6W steel, 133
- in situ* fracture experiment on a duplex stainless steel, 157
- on the cavity-growth-model-based prediction of the stress dependence of time to creep fracture, L5
- the fracture resistance of sintered steel, 149

Graphite

- a high resolution transmission electron microscopy study of SiC-coated graphite fiber-aluminum composite, 199

Hardening

- the strain hardening behaviour of dual-phase steel, 67

Hydrogen

- effect of directional solidification on resistance to hydrogen embrittlement of a stainless steel, 221
- plastic deformation: a major factor in hydrogen embrittlement of low alloy steel, L11

Iron

- crystallization of low silicon content Fe-Si-B metallic glasses, 255
- mechanical properties of Fe-30Mn-10Al-1C-1Si alloy, 141
- rapid solidification and self-annealing of Fe-C-Si alloys by low pressure plasma spraying, 207
- rapidly solidified thick deposit layers of Fe-C-Mo alloys by flame spraying, 227

Layered structures

- extended X-ray absorption fine structure of interfaces of layered structures, 45

Magnesium

- characterization of submicrometer phase particles in rapidly solidified Mg-20Nd, 11
- the mechanism of superplastic flow in an Al-Mg alloy, L31

Manganese

- mechanical properties of Fe-30Mn-10Al-1C-1Si alloy, 141

Martensite

- effects of nickel additions on the fracture behavior of tempered martensite in medium-carbon 6W steel, 133
- up-quenching effect on the stabilization process of a Cu-Zn-Al martensite, 247

Mechanical properties

- mechanical properties of Fe-30Mn-10Al-1C-1Si alloy, 141

Metallic glasses

- crystallization of low silicon content Fe-Si-B metallic glasses, 255

Molybdenum

- rapidly solidified thick deposit layers of Fe-C-Mo alloys by flame spraying, 227
- resistometric study of short-range ordering in Ni-10at.%Mo, L17

Nanocrystalline materials

- nanocrystalline materials, 33

Neodymium

- characterization of submicrometer phase particles in rapidly solidified Mg-20Nd, 11

Nickel

- effects of nickel additions on the fracture behavior of tempered martensite in medium-carbon 6W steel, 133
- morphology of zirconia in Y-PSZ sintered with Ni₂AlTi, 191
- phase transformations in (Ni,Cu)₃Sn alloys, 167
- resistometric study of short-range ordering in Ni-10at.%Mo, L17

Niobium

- electron microscopy observation of an *in situ* Cu-Nb composite, 59

Nitrogen

- preparation of the metastable interstitial copper nitride, Cu₄N, by d.c. plasma ion nitriding, L1

Phase transformations

- phase transformations in (Ni,Cu)₃Sn alloys, 167

Precipitation

- coherent precipitation of M₂C carbides in AF1410 steel, 215
- the effect of cold work on the precipitation kinetics of an advanced austenitic steel, 235

Quenching

- up-quenching effect on the stabilization process of a Cu-Zn-Al martensite, 247

Rapid solidification

- characterization of submicrometer phase particles in rapidly solidified Mg-20Nd, 11
- rapid solidification and self-annealing of Fe-C-Si alloys by low pressure plasma spraying, 207
- rapid solidification of lightweight metal alloys, 19
- rapidly solidified thick deposit layers of Fe-C-Mo alloys by flame spraying, 227

Short-range ordering

- resistometric study of short-range ordering in Ni-10at.%Mo, L17

Silicon

- a high resolution transmission electron microscopy study of SiC-coated graphite fiber-aluminum composite, 199
- crystallization of low silicon content Fe-Si-B metallic glasses, 255
- dynamic strain aging in Czochralski-grown silicon single crystals, 75
- mechanical properties of Fe-30Mn-10Al-1C-1Si alloy, 141
- rapid solidification and self-annealing of Fe-C-Si alloys by low pressure plasma spraying, 207

Silver

- some correlations between parameters relating to grain boundary self-diffusion in silver, L21

Sintering

morphology of zirconia in Y-PSZ sintered with Ni_2AlTi , 191

the fracture resistance of sintered steel, 149

Slip

control of intergranular fatigue cracking by slip homogeneity in copper

I: effect of grain size, 95

II: effect of loading mode, 103

on the orientation of cyclic-slip-induced intergranular fatigue cracks in face-centred cubic metals, L21

Solidification

effect of directional solidification on resistance to hydrogen embrittlement of a stainless steel, 221

Stainless steel

effect of directional solidification on resistance to hydrogen embrittlement of a stainless steel, 221

in situ fracture experiment on a duplex stainless steel, 157

Strain

dynamic strain aging in Czochralski-grown silicon single crystals, 75

the strain hardening behaviour of dual-phase steel, 67

Stress

elastic stress transfer from fiber to coating in a fiber-coating system, 115

on the cavity-growth-model-based prediction of the stress dependence of time to creep fracture, L5

structures and stresses in nanograin thin metal films, 3

Superplastic flow

the mechanism of superplastic flow in an Al-Mg alloy, L31

Tempering

investigation into the structural evolutions of a low alloy steel during tempering, 175

Thermal expansion

the thermal expansion of a two-phase composite with body-centred cubic symmetry, 125

Thin films

structures and stresses in nanograin thin metal films, 3

Tin

phase transformations in $(\text{Ni,Cu})_3\text{Sn}$ alloys, 167

Titanium

morphology of zirconia in Y-PSZ sintered with Ni_2AlTi , 191

Transmission electron microscopy

a high resolution transmission electron microscopy study of SiC-coated graphite fiber-aluminum composite, 199

Tungsten

effects of nickel additions on the fracture behavior of tempered martensite in medium-carbon 6W steel, 133

Y-PSZ

morphology of zirconia in Y-PSZ sintered with Ni_2AlTi , 191

Zinc

up-quenching effect on the stabilization process of a Cu-Zn-Al martensite, 247

Zirconia

morphology of zirconia in Y-PSZ sintered with Ni_2AlTi , 191

THE UNIVERSITY OF CHICAGO

PHYSICS DEPARTMENT

1955-1956

PHYSICS 301

LECTURE NOTES

BY

ROBERT H. FERRY

PHYSICS DEPARTMENT

UNIVERSITY OF CHICAGO

CHICAGO, ILLINOIS

1956

